Active Fault Management for Networked Microgrids

Wenfeng Wan, *Student Member, IEEE*, Yan Li, *Student Member, IEEE*, Bing Yan, *Member, IEEE*, Mikhail A. Bragin, *Member, IEEE*, Jason Philhower, *Senior Member, IEEE*, Peng Zhang, *Senior Member, IEEE*, and Peter B. Luh, *Life Fellow, IEEE*

***Abstract*—This paper presents Active Fault Management for Networked Microgrids (AFM-NM) to manage microgrids during faults. Two challenges remain in NMs' fault management. The first one is a lack of panoramic management schemes that allow easy change of objectives and constraints as needed rather than fixed on certain objectives and constraints. The second challenge is the implementation of distributed management for NWs under fault conditions instead of normal conditions. The two challenges are addressed in the presented AFM-NM. First, AFM-NM is formulated as an online optimization problem so that customized objectives and constraints can be conveniently added to the formulation, e.g., power ripples and balance, and fault current levels and contribution. Second, the coordination of each microgrid' AFM is enabled by the Surrogate Lagrangian Relaxation (SLR) method to allow distributed computation with guaranteed convergence. Comparison results with a conventional ride-through method show AFM-NM achieves desirable trade-offs between different objectives. Comparison with centralized AFM demonstrates distributed AFM-NM ensures convergence and accuracy.**

***Keywords*—active fault management (AFM), networked microgrids (NMs), faults, ride through, Surrogate Lagrangian Relaxation (SLR)**

I. Introduction

NETWORKED microgrids (NMs) are able to provide resiliency benefits by sharing power during extreme events and further improving reliability for critical loads [1], [2]. One major issue, however, is fault management in NMs. Fault management enables microgrids to ride through faults, to maintain microgrids' operation and to support the main grid's recovery [3], [4]. One challenge of fault management is that microgrids could contribute large currents into the main grid, exceeding the designed fault level and thus damaging utility equipment. Further, the undesirable occurance of double-frequency power ripples, if not managed, significantly compromise the reliability of converters and storages [5].

Another challenge of NMs' fault managment is achievement of convergent coordination among a cluster of individual microgrids. Without convergent coordination, it is usually beyond one microgrid's capability to meet control objectives, e.g., fault currents contribution and power balance, since other microgrids' output currents would potentially counteract that single microgrid's effort.

This work was supported in part by the National Science Foundation under Grants ECCS-1611095, CNS-1647209 and ECCS-1831811, and in part by the Office of the Provost, University of Connecticut.

W. Wan, Y. Li, B. Yan, M. A. Bragin, J. Philhower, P. Zhang, and P. B. Luh are with the Department of Electrical and Computer Engineering, University of Connecticut, Storrs, CT 06269, USA (e-mail: peng.zhang@uconn.edu).

Many strategies have been published to manage microgrids during faults. Even though adding hardware, e.g., current limiters [6], can effectively reduce fault currents and transients, this method improves cost and doesn't fully take advantage of flexibility of microgrids' converters. Virtual-Impedance method [7] has been adopted to limit output currents of microgrids, but whether microgrids would increase the fault current level in the main grid is not studied. To ensure the fault current levels in the main grid are unchanged after the integration of microgrids, the phase angles of microgrids' currents are managed in [8]. However, only the fault current contribution is considered, while the effect of other variables, e.g., power ripples and power balance, are not considered.

Similar to the above methods to reduce fault currents, converters have also been leveraged to reduce double-line-frequency power ripples during faults. Double synchronous reference frame vector control and stationary frame control with proportional-resonant controllers are two widely used methods to reduce power ripples in grid-connected converters [9]. These two methods only focus on the operation of converters and renewable generation, while the effect on the main grid with regard to fault current level and power balance are not investigated.

Distributed management scheme is emerging for the coordination of microgrids, such as voltage and frequency regulation, generation-consumption scheduling and supple-demand mismatch control [10], largely because of the nature of information inaccessibility between microgrids. So far, only microgrids' normal operation has been studied and few work has designed distributed approaches for NMs' fault management. A major challenge in the existing designs is that they are unable to consider the effect of the dynamics in the neighboring microgrids.

To bridge the gaps, this paper presents an active fault management for networked microgrids (AFM-NM). Novelties of this paper are twofold. First, AFM-NM is formulated as an online optimization problem which is modular and plug-and-play, meaning additional variables e.g., power, currents and voltages from existing and future microgrids, can be added to the objectives and constraints as needed. Second, an efficient and reliable surrogate lagrangian relaxation (SLR) method [11] is offered as an AFM-NM solver, which has theoretically guaranteed convergence. Simulation results have demonstrated the convergence and efficacy of the SLR-enabled AFM-NM, while the desirable trade-offs between different objectives during fault management are achieved by the combination of Pareto frontier and feedback control.

978-1-7281-1981-6/19/$31.00 ©2019 IEEE

II. Problem Formulation

Without loss of generality, AFM-NM for N interconnected microgrids (Fig. 1) is formulated by an optimization problem. This new conceptual AFM-NM is flexible, because interested variables can be added to the formulation's objectives and constraints as needed.

Formulation equations are expressed in the rectangular coordinate system, in which root mean square voltages and currents are expressed as,

$$\begin{cases} \mathbf{U_p} = U_{px} + jU_{py} \\ \mathbf{I_p} = I_{px} + jI_{py} \end{cases} \quad p = a, b, c \tag{1}$$

The objective in (2) contains two parts: O_1 and O_2. O_1 represents how much microgrids contribute to increasing the main grid's fault currents. O_2 represents the double-line-frequency ripples in microgrids' output power. $I_{px}^{mi}, I_{py}^{mi} (p = a, b, c; i = 1, ...N)$ are $6N$ variables to be computed.

minimize

$$\beta O_1 + (1 - \beta) O_2, \quad \beta \in [0, 1] \tag{2}$$

$$\begin{cases} O_1 \equiv \frac{1}{C_1} \sum_k \left| (I_{kx}^M + I_{kx}^m)^2 + (I_{ky}^M + I_{ky}^m)^2 - (I_{kx}^M)^2 - (I_{ky}^M)^2 \right| \\ O_2 \equiv \frac{1}{C_2} \sum_i \frac{D_i}{(P_i)^2} \\ I_{kx}^m \equiv \sum_i (l_{T1\_i} I_{kx}^{mi} + l_{T2\_i} I_{ky}^{mi}) \\ I_{ky}^m \equiv \sum_i (l_{T3\_i} I_{kx}^{mi} + l_{T4\_i} I_{ky}^{mi}) \\ D_i \equiv [\sum_p (U_{px}^{mi} I_{px}^{mi} - U_{py}^{mi} I_{py}^{mi})]^2 + [\sum_p (U_{py}^{mi} I_{px}^{mi} - U_{px}^{mi} I_{py}^{mi})]^2 \end{cases}$$
$$i = 1, ..., N; \quad p = a, b, c; \quad k = a, b, c \tag{3}$$

subject to

$$\sum_p (U_{px}^{mi} I_{px}^{mi} + U_{py}^{mi} I_{py}^{mi}) = P_i \quad i = 1, ..., N; p = a, b, c \tag{4}$$

$$\begin{cases} I_{ax}^{mi} + I_{bx}^{mi} + I_{cx}^{mi} = 0 \\ I_{ay}^{mi} + I_{by}^{mi} + I_{cy}^{mi} = 0 \end{cases} \quad i = 1, ..., N \tag{5}$$

$$\begin{cases} (I_{ax}^{mi})^2 + (I_{ay}^{mi})^2 \le (I_{rate}^{mi})^2 \\ (I_{bx}^{mi})^2 + (I_{by}^{mi})^2 \le (I_{rate}^{mi})^2 \\ (I_{cx}^{mi})^2 + (I_{cy}^{mi})^2 \le (I_{rate}^{mi})^2 \end{cases} \quad i = 1, ..., N \tag{6}$$

$$\begin{cases} (\sum_i I_{ax}^{mi})^2 + (\sum_i I_{ay}^{mi})^2 \le (I_{rate}^M)^2 \\ (\sum_i I_{bx}^{mi})^2 + (\sum_i I_{by}^{mi})^2 \le (I_{rate}^M)^2 \\ (\sum_i I_{cx}^{mi})^2 + (\sum_i I_{cy}^{mi})^2 \le (I_{rate}^M)^2 \end{cases} \quad i = 1, ..., N \tag{7}$$

where i represents microgrid i. The total number of microgrids is N. p represents all three phases: a, b, c. k represents faulted phases. If phases a and b encounter ground faults, then k is a and b. The superscripts M, mi represent variables from the main grid and microgrid i, respectively. The superscripts m represents total values from all the microgrids. The subscripts x, y represent x-axis component and y-axis component in the rectangular coordinate system, respectively.

The weight factor β is the trade-offs between O_1 and O_2 and its value is decided by Pareto frontier. C_1 and C_2 are scale factors to make O_1 and O_2 in the same order to ensure computation accuracy. Constants $l_{T1\_i}, l_{T2\_i}, l_{T3\_i}, l_{T4\_i}$ represent the effect of transformers on microgrid i' currents. P_i is microgrid i's output power before faults. I_{rate}^M and I_{rate}^{mi} are the safety current ratings of the main grid and microgrid i, respectively.

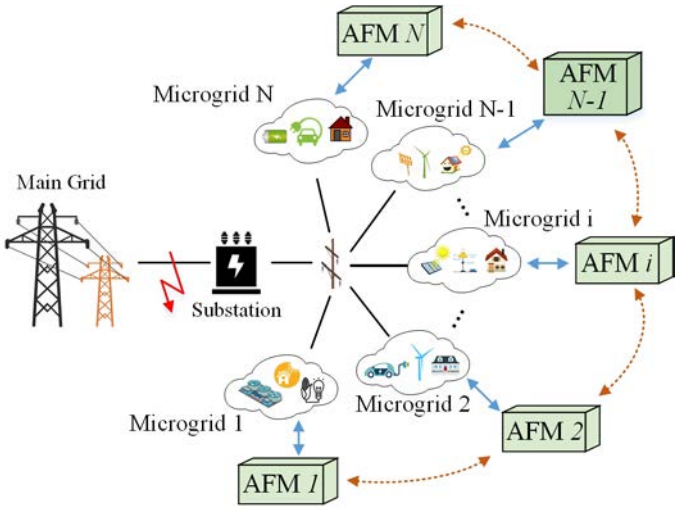

Fig. 1. Schematic of AFM for networked microgrids (AFM-NM).

For the objective (2), $\sqrt{(I_{kx}^M + I_{kx}^m)^2 + (I_{ky}^M + I_{ky}^m)^2}$, $\sqrt{(I_{kx}^M)^2 + (I_{ky}^M)^2}$, $\sqrt{(I_{kx}^m)^2 + (I_{ky}^m)^2}$ are the total fault currents, fault currents from the main grid and fault currents from microgrids measured at the fault location, respectively. $\sqrt{D_i}$ is microgrid i's power ripples. In the formulation, the square roots are removed to improve computation speed.

For the constraints, (4) is power balance before and after faults to avoid instability induced by sudden change of power transfer. (5) is to eliminate zero-sequence components. (6) and (7) are safety current ratings for the microgrid i and the main grid, respectively.

III. Methods: Surrogate Lagrangian Relaxation

Within SLR, after relaxation of constraint (7) that couples N microgrids, the resulting relaxed problem is decomposed into N subproblems [11], each subproblem belonging to each microgrid's AFM.

The subproblem for microgrid i's AFM is formulated in (8)-(13). The decision variables are $I_{px}^{mi}, I_{py}^{mi} (p = a, b, c)$, which are microgrid i's three-phase output currents expressed in the rectangular coordinate system.

minimize

$$\beta O_1^{mi} + (1 - \beta) O_2^{mi} + \lambda_1 g_1 + \lambda_2 g_2 + \lambda_3 g_3, \beta \in [0, 1] \tag{8}$$

$$\begin{cases} O_1^{mi} \equiv \frac{1}{C_1} \sum_k \left| (I_{kx}^M + I_{kx}^m)^2 + (I_{ky}^M + I_{ky}^m)^2 - (I_{kx}^M)^2 - (I_{ky}^M)^2 \right| \\ O_2^{mi} \equiv \frac{1}{C_{2\_i}} \frac{D_i}{(P_i)^2} \\ I_{kx}^m \equiv \sum_i (l_{T1\_i} I_{kx}^{mi} + l_{T2\_i} I_{ky}^{mi}) \\ I_{ky}^m \equiv \sum_i (l_{T3\_i} I_{kx}^{mi} + l_{T4\_i} I_{ky}^{mi}) \\ D_i \equiv [\sum_p (U_{px}^{mi} I_{px}^{mi} - U_{py}^{mi} I_{py}^{mi})]^2 + [\sum_p (U_{py}^{mi} I_{px}^{mi} - U_{px}^{mi} I_{py}^{mi})]^2 \end{cases}$$
$$p = a, b, c; \quad k = a, b, c \tag{9}$$

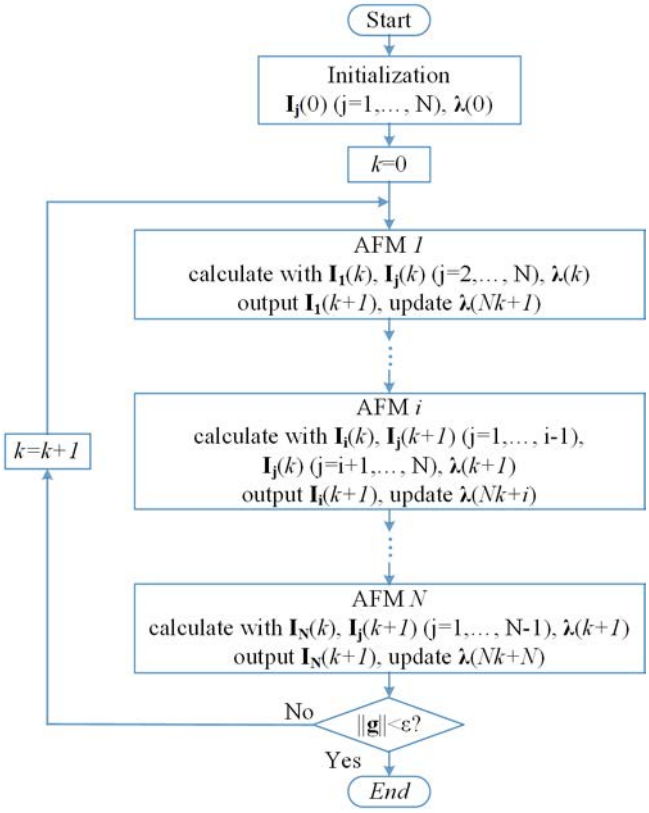

Fig. 2. SLR's computation process. The convergence criterion is norm of (g_1, g_2, g_3) being smaller than a threshold

$$\begin{cases} g_1 \equiv (\sum_s I_{ax}^{ms})^2 + (\sum_s I_{ay}^{ms})^2 - (I_{rate}^{M})^2 \\ g_2 \equiv (\sum_s I_{bx}^{ms})^2 + (\sum_s I_{by}^{ms})^2 - (I_{rate}^{M})^2 \\ g_3 \equiv (\sum_s I_{cx}^{ms})^2 + (\sum_s I_{cy}^{ms})^2 - (I_{rate}^{M})^2 \end{cases} \quad s = 1, ..., N \tag{10}$$

subject to

$$\sum_p (U_{px}^{mi} I_{px}^{mi} + U_{py}^{mi} I_{py}^{mi}) = P_i \quad p = a, b, c \tag{11}$$

$$\begin{cases} I_{ax}^{mi} + I_{bx}^{mi} + I_{cx}^{mi} = 0 \\ I_{ay}^{mi} + I_{by}^{mi} + I_{cy}^{mi} = 0 \end{cases} \tag{12}$$

$$\begin{cases} (I_{ax}^{mi})^2 + (I_{ay}^{mi})^2 \le (I_{rate}^{mi})^2 \\ (I_{bx}^{mi})^2 + (I_{by}^{mi})^2 \le (I_{rate}^{mi})^2 \\ (I_{cx}^{mi})^2 + (I_{cy}^{mi})^2 \le (I_{rate}^{mi})^2 \end{cases} \tag{13}$$

where g_1, g_2, g_3 are violations levels of the relaxed constraint (7). $\lambda_1, \lambda_2, \lambda_3$ are three Lagrange multipliers, corresponding to g_1, g_2, g_3, respectively. C_{2_i} is a scale factor to ensure accurate calculation. All the other symbols have the same meanings as in (2)-(7).

Fig. 2 gives the computation process of SLR. During AFM i's computation, other microgrids' output, i.e., $I_{px}^{mi}, I_{py}^{mi} (p = a, b, c; i = 1, ..., i-1, i+1, ..., N)$, are considered unchanged. Lagrangian multipliers $\boldsymbol{\lambda}$ are updated after each microgrid finishes its computation and would be updated N times for an iteration. The proof for SLR's convergence and the method

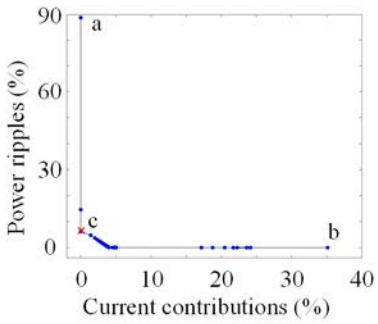

Fig. 3. Pareto frontier for networked microgrids' AFM during single-phase-to-ground fault.

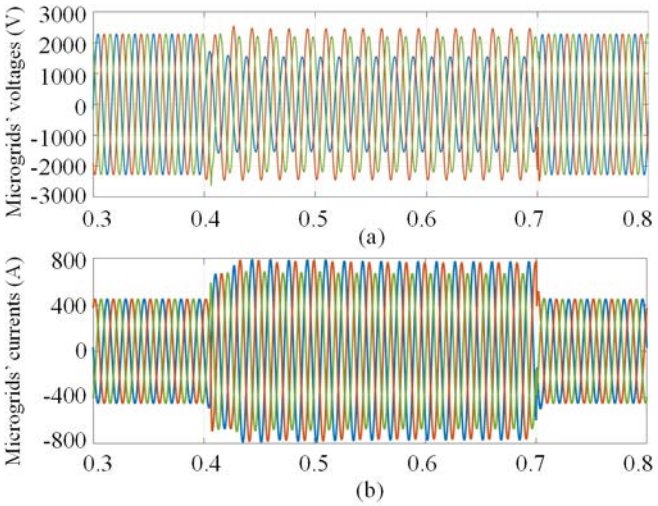

Fig. 4. Simulation results for single-phase-to-ground faults with distributed AFM-NM. (a) Grid-connected converters' output voltages; (b) Total output currents of two microgrids.

for updating Lagrangian multipliers $\boldsymbol{\lambda}$ are given in [11]. Compared with the centralized formulation (2)-(7), the SLR method' formulation (8)-(13) is distributed and has advantages of extensibility and flexibility.

IV. Case Study

The designed distributed AFM-NM has been verified with Matlab/Simulink simulation. The simulation results have been compared with results of a conventional ride-through method and results of centralized AFM.

A. System Description

In the studied system, two microgrids are considered and both of them connect to the main grid through grid-connected converters (GCC). Resistive faults are simulated to occur at the main grid. Before faults, there is no current flow through the faulted lines, which simulates the situation where some loads in the main grid are powered by microgrids' excessive power. Microgrid 1 and microgrid 2 deliver 0.91 MW and 0.66 MW to the main grid, respectively, without any reactive power transfer. The voltage rating of the transformer between

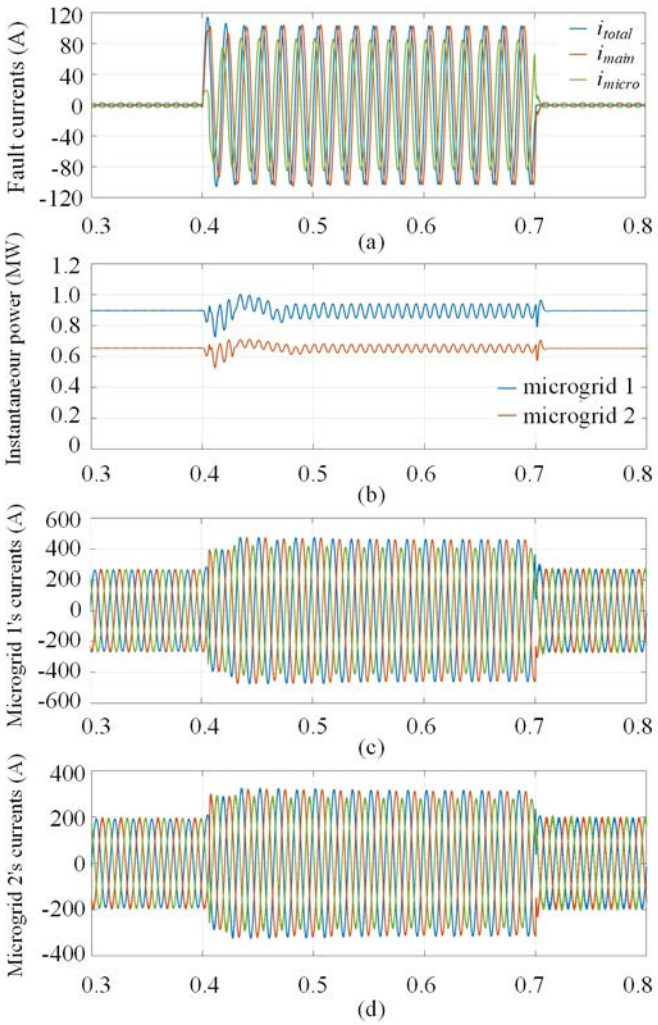

Fig. 5. Simulation results for distributed AFM-NM. (a) Fault currents at fault location. i_{total} is the total fault currents to the ground, i_{main} is fault currents from the main grid, i_{micro} is fault currents from both microgrids; (b) Instantaneous active power of two microgrids; (c) Microgrid 1's output currents; (d) Microgrid 2's output currents.

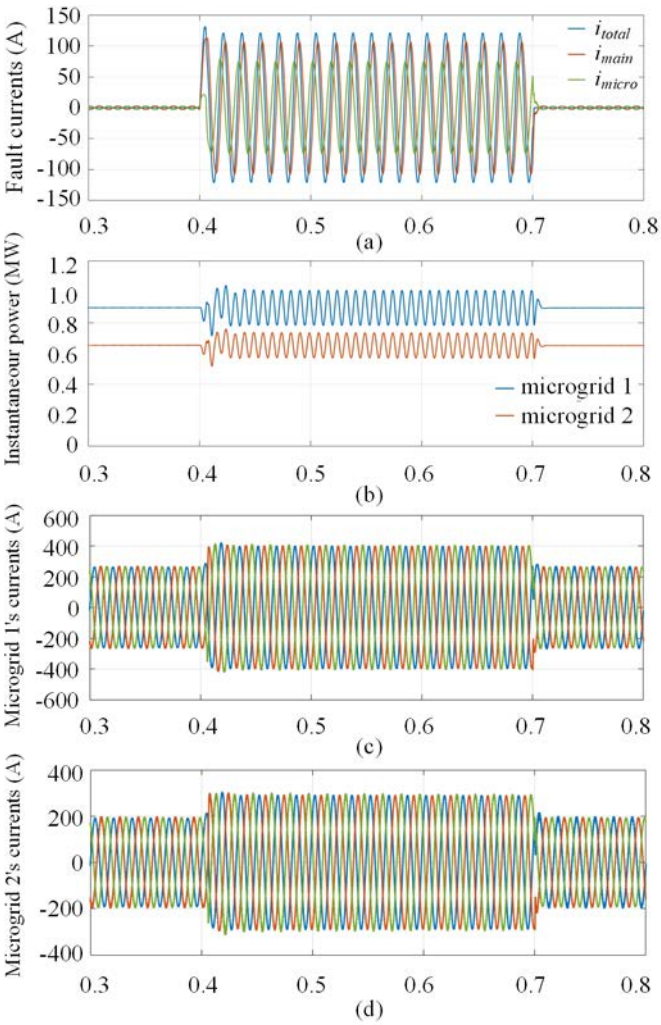

Fig. 6. Simulation results without AFM. (a) Fault currents at fault location. i_{total} is the total fault currents to the ground, i_{main} is fault currents from the main grid, i_{micro} is fault currents from both microgrids; (b) Instantaneous active power of two microgrids; (c) Microgrid 1's output currents; (d) Microgrid 2's output currents.

the main grid and microgrids is 27:2.9 kV. Fault currents from the main grid and microgrids, and the total fault currents are measured. Microgrids' instantaneous power are also measured.

B. Single-phase-to-ground Fault

Single-phase-to-ground fault is studied here. The general formulation (2)-(7) and the SLR method (8)-(13) are also applicable to other types of faults. As shown in (2) and (8), the weight factor β needs to be determined first, representing the trade-offs between fault current contribution (O_1) and power ripples (O_2). Pareto frontier is able to provide the best possible trade-offs between different objectives. The Pareto frontier for the single-phase-to-ground fault of NMs is given in Fig. 3. Points a and b represent two extreme cases, corresponding to $\beta = 1$ and $\beta = 0$, respectively. Point c with coordinates of $(0.00\%, 5.35\%)$ is chosen as the operation point during faults. It means the fault current contribution and power ripples are chosen to be controlled as 0.00% and 5.35%, respectively. Other operation points can be chosen from the Pareto frontier.

Both AFMs compute with interior-point methods. During AFM 1's computation, (8)-(13), variables from AFM 2, $I^{m2}_{px}, I^{m2}_{py} (p = a, b, c)$, are considered constant. During AFM 2's computation, also (8)-(13) , variables from AFM 1, $I^{m1}_{px}, I^{m1}_{py} (p = a, b, c)$, are considered constant. As shown in Fig. 2, Lagrangian multipliers are updated after each AFM's calculation to improve convergence speed.

The simulation results are shown in Fig. 4 and 5. Phase a is the fault phase and the remainging voltage is $0.7\ pu$. The fault occurs at 0.4s and is cleared at 0.7s. $I^{M}_{rate}, I^{m1}_{rate}$ and I^{m2}_{rate} are set to be $\frac{800}{\sqrt{2}}A$, $\frac{600}{\sqrt{2}}A$ and $\frac{400}{\sqrt{2}}A$, respectively. As given in the results, two microgrids' output currents and their sum are within safety current ratings. Fig. 5 (a) are fault currents from

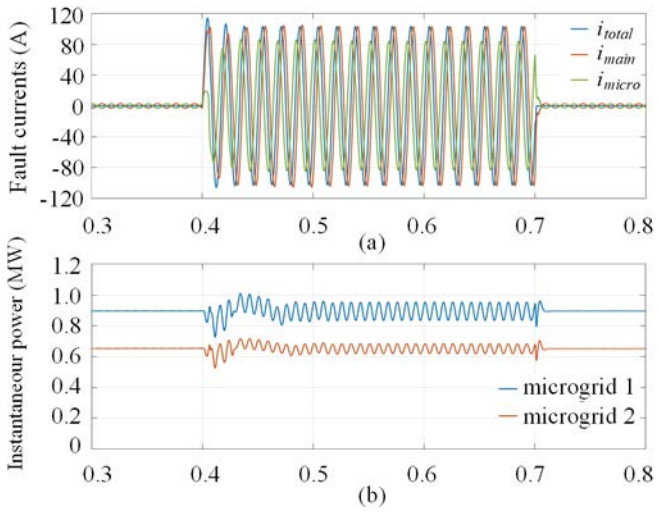

Fig. 7. Simulation results with centralized AFM. (a) fault currents at fault location. i_{total} is the total fault currents to the ground, i_{main} is fault currents from the main grid, i_{micro} is fault currents from both microgrids; (b) Instantaneous active power of two microgrids.

the main grid, microgrids and currents to the ground. Fig. 5 (b) are two microgrids' output instantaneous power. According to Fig. 5 (a) and (b), the current contribution and power ripples are managed to be 0.00% and 4.77%, respectively, close to values $(0.00\%, 5.35\%)$ given by the Pareto frontier.

C. Comparison with Conventional Ride-through Method

This conventional ride-through method controls power balance and GCCs' DC voltages. It also considers safety current ratings I^M_{rate}, I^{m1}_{rate} and I^{m2}_{rate}, but doesn't consider microgrids' contribution of improving fault current level or output power's ripples. Fig. 6 are the simulation results for the conventional ride-through method. The current contribution and power ripples are 13.55% and 12.77%, respectively, both of which are worse than the results of AFM. It should be noted that only two microgrids are studied in this paper. If more microgrids are connected to the main grid, the current contribution would be much worse with the conventional ride-through method.

D. Comparison with Centralized AFM

In centralized AFM, all the microgrids share one AFM modular. Because it can collect data from all the microgrids, centralized AFM can guarantee convergence without iterations. Fig. 7 are the simulation results for centralized AFM. The current contribution and power ripples are 0.00% and 5.75%, respectively, close to the results of 0.00% and 4.77% for distributed AFM. This proves the distributed AFM is convergent and is as accurate as centralized AFM. It should be emphasized that centralized AFM is not suitable for NMs because of microgrids' distributed nature. Table I gives the comparison of different fault managment methods.

V. Conclusion

Active Fault Management for Networked Microgrids (AFM-NM) to manage NMs is established, allowing microgrids to continue contributing power and ancillary support during grid faults. AFM-NM is formulated as an optimization problem so that customized objectives and constraints can be easily added. Also, the distributed computation of AFM for NMs is achieved with the Surrogate Lagrangian Relaxation (SLR) method. Case-study results show that AFM-NM can get better trade-offs between different objectives than the conventional ride-through method and are as accurate as centralized methods. AFM-NM can be incorporated into microgrids' secondary control without extra hardware. Integration of AFM-NM with other research is promising, such as stability and reconfiguration of microgrids. The basic idea of AFM-NM with distributed optimization can also be applied to other types of grids, e.g., DC and AC/DC grids. In the future, more microgrids connected to large-scale systems and asynchronous AFMs would be studied.

TABLE I
Comparison among different fault management methods

Methods	Fault current contribution	Power ripples
Distributed AFM	0.00%	4.77%
Conventional ride-through method	13.55%	12.77%
Centralized AFM	0.00%	5.75%

References

[1] Y. Li, P. Zhang, and P. B. Luh, "Formal analysis of networked microgrids dynamics," *IEEE Transactions on Power Systems*, vol. 33, no. 3, pp. 3418–3427, 2018.

[2] Y. Li, P. Zhang, M. Althoff, and M. Yue, "Distributed formal analysis for power networks with deep integration of distributed energy resources," *IEEE Transactions on Power Systems*, 2018.

[3] W. Wan, Y. Li, B. Yan, M. A. Bragin, J. Philhower, P. Zhang, P. B. Luh, and G. Warner, "Active fault management for microgrids," in *44th Annual Conference of the IEEE Industrial Electronics Society (IECON)*, October 2018, pp. 1–6.

[4] *IEEE Std 1547-2018: IEEE Standard for Interconnection and Interoperability of Distributed Energy Resources with Associated Electric Power Systems Interfaces*, April 2018.

[5] H. C. Chen, S. H. Li, and C. M. Liaw, "Switch-mode rectifier with digital robust ripple compensation and current waveform controls," *IEEE Transactions on Power Electronics*, vol. 19, no. 2, pp. 560–566, 2004.

[6] T. Ghanbari and E. Farjah, "Unidirectional fault current limiter: An efficient interface between the microgrid and main network," *IEEE Transactions on Power Systems*, vol. 28, no. 2, pp. 1591–1598, May 2013.

[7] H. R. Baghaee, M. Mirsalim, and G. B. Gharehpetian, "Real-time verification of new controller to improve small/large-signal stability and fault ride-through capability of multi-der microgrids," *IET Generation, Transmission & Distribution*, vol. 10, no. 12, pp. 3068–3084, 2016.

[8] N. Rajaei, M. H. Ahmed, M. M. Salama, and R. K. Varma, "Fault current management using inverter-based distributed generators in smart grids," *IEEE Transactions on Smart Grid*, vol. 5, no. 5, pp. 2183–2193, 2014.

[9] A. Junyent-Ferre, O. Gomis-Bellmunt, T. C. Green, and D. E. Soto-Sanchez, "Current control reference calculation issues for the operation of renewable source grid interface vscs under unbalanced voltage sags," *IEEE Transactions on Power Electronics*, vol. 26, no. 12, pp. 3744–3753, Dec 2011.

[10] A. R. Malekpour and A. Pahwa, "Stochastic networked microgrid energy management with correlated wind generators," *IEEE Transactions on Power Systems*, vol. 32, no. 5, pp. 3681–3693, Sept 2017.

[11] M. A. Bragin, P. B. Luh, J. H. Yan, N. Yu, and G. A. Stern, "Convergence of the surrogate lagrangian relaxation method," *Journal of Optimization Theory and Applications*, vol. 164, no. 1, pp. 173–201, Jan 2015.